

Optical delay control of large-spectral-bandwidth laser pulses

Emilio Ignesti¹, Stefano Cavalieri^{2,3}, Lorenzo Fini^{2,3,*}, Emiliano Sali^{2,3,*},

Marco V. Tognetti¹, Roberto Eramo^{2,3,4} and Roberto Buffa¹

¹*Dipartimento di Fisica, Università di Siena,
Via Roma 56, I-53100 Siena, Italy.*

²*Dipartimento di Fisica,
Università di Firenze, Via G. Sansone 1,
I-50019 Sesto Fiorentino, Firenze, Italy.*

³*European Laboratory for Non-Linear Spectroscopy (LENS),
Università di Firenze,
Via N. Carrara 1, I-50019 Sesto Fiorentino, Firenze, Italy.*

⁴*INFN-CRS-Soft Matter (CNR),
c/o Università la Sapienza,
Piazzale A. Moro 2, I-00185, Roma, Italy.*

*Corresponding author: sali@fi.infn.it

In this letter we report the first experimental observation of temporal delay control of large-spectral-bandwidth multimode laser pulses by means of electromagnetically induced transparency (EIT). We achieved controllable retardation with limited temporal distortion of optical pulses with an input spectral bandwidth of 3.3 GHz. The experimental results compare favorably with theoretical predictions.

In recent years the number of experiments aiming at the reduction of the group velocity of laser pulses propagating through material media has been growing steadily. The interest in this research field concerns both fundamental issues (basic physical laws of laser-matter interaction) and applications to all-optical technologies. Many schemes have been proposed and experimentally realized, based on effects such as electromagnetically induced transparency (EIT) [1], coherent population oscillations [2, 3], stimulated Brillouin and Raman scattering [4, 5, 6, 7, 8], spectral hole burning [9] and double absorbing resonances [10, 11]. The possibility to coherently control not only the propagation velocity of laser pulses, but also their temporal shape [12], probably makes systems based on EIT the most promising for the design of all-optical delay lines and buffers with very fast temporal switching. So far, experimental observation of controllable temporal delay by means of EIT has been reported only for narrowband Fourier-transform-limited optical pulses, where the spectral bandwidth $\delta\omega$ is inversely proportional to the pulse temporal duration δt . However, such condition is not strictly necessary in digital optical communications. Therefore, in order to study the limitations of techniques based on EIT, it appears of evident interest to investigate also the possibility of temporal delay control of multimode non Fourier-transform-limited laser pulses.

In this letter we report what, to the best of our knowledge, is the first experimental observation of delay control by EIT of large-spectral-bandwidth multimode dye laser pulses. We show how EIT holds the potential to achieve controllable retardation of laser pulses with a spectral bandwidth as large as 3.3 GHz.

Figure 1 shows our experimental apparatus and, in the top-left inset, the atomic levels and the transitions involved. The three-level ladder scheme in sodium in-

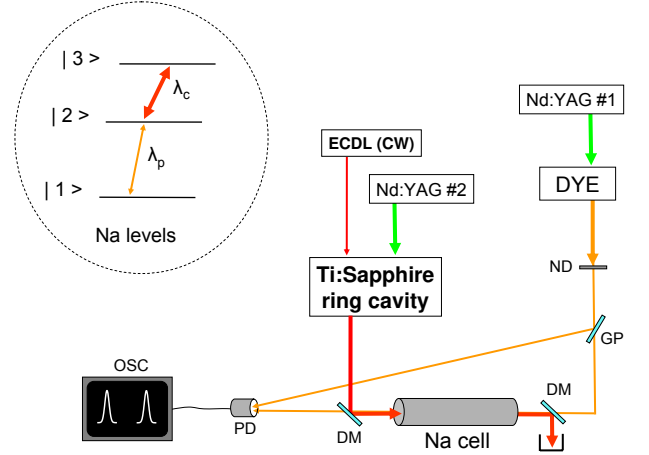


FIG. 1: Experimental setup. ECDL: extended-cavity diode laser. ND: neutral-density filter. DM: dichroic mirror. GP: glass plate. PD: photo-diode. OSC: Digital oscilloscope. Top-left inset: scheme of sodium levels involved.

volves the atomic states $|1\rangle = |2p^63s\ J = 1/2\rangle$, $|2\rangle = |2p^63p\ J = 1/2\rangle$ and $|3\rangle = |2p^63d\ J = 3/2\rangle$. The probe field at $\lambda_p \simeq 589.76$ nm, resonant with the transition $|1\rangle - |2\rangle$, is provided by a commercial frequency-tunable multimode dye laser (Quantel TDL50) pumped by a frequency-doubled Q-switched Nd:YAG laser at a repetition rate of 10 Hz. The dye laser pulses have a measured spectral bandwidth $\delta\omega/2\pi = 3.3$ GHz and a multi-peak temporal structure of several nanoseconds of duration. The temporal evolution of a typical laser pulse is reported in Fig. 2(a). The coupling field at $\lambda_c \simeq 818.55$ nm, resonant with the transition $|2\rangle - |3\rangle$, is provided by a home-made laser, since no commercially available devices exist with the required characteristics,

i.e. frequency tunability, single-longitudinal-mode operation (for temporal smoothness) and adjustable pulse duration. The choice was that of a titanium-sapphire (Ti:S) ring cavity pumped by another frequency-doubled Q-switched Nd:YAG laser and injection-seeded by a Topica DL100 single-mode CW extended-cavity diode laser (ECDL) [13]. The single-mode emission of the ECDL can be tuned in wavelength within the emission bandwidth of the diode laser (typically a few nm). Both the wavelength of the CW injection-seed from the ECDL and the wavelength of the pulsed emission from the Ti:S cavity are monitored using a high-diffraction-order spectrometer (Coherent Wavemaster) with an accuracy of 5 pm. The sodium sample is contained in a cylindrical cell, heated up to several hundreds degree Celsius for a length $L = 1$ m. All measurements have been carried out at a temperature of 250° Celsius, corresponding to an independently measured value of the density-length product of $2.0 \times 10^{15} \text{ cm}^{-2}$. The two laser beams are linearly polarized along the same direction and they overlap, both temporally and spatially, inside the cell. A counter-propagating configuration was arranged in order for the effect of Doppler broadening to be reduced. The temporal synchronization of the laser pulses was obtained by mutually adjusting the triggers of the two Nd:YAG pump lasers. The length of the ring cavity of the control laser was chosen in such a way to obtain a pulse temporal duration much longer than that of the probe pulse. For a cavity length of 145 cm a temporal duration full-width at half-maximum (FWHM) for the control pulse of 62 ns was obtained. For such a value, the control field can be considered sufficiently constant in time upon propagation of the laser pulses along the cell. The probe beam has a slightly elliptical profile with a 2-mm mean diameter, while the overlapping control beam has a homogeneous circular profile with a 4-mm diameter.

All the measurements have been done with a probe pulse energy $E_p \simeq 30$ nJ, corresponding to a peak intensity inside the cell of approximately $I_p \sim 100 \text{ W/cm}^2$, while, in order to obtain various delays, we have varied the energy of the control pulse from $E_c \simeq 0.3$ mJ to $E_c \simeq 7$ mJ, corresponding to peak intensities inside the cell varying from $I_c \simeq 30 \text{ kW/cm}^2$ to $I_c \simeq 700 \text{ kW/cm}^2$. The detection system is constituted by a fast photodiode (Antel Opttronix PIN) and a digital sampling oscilloscope (Tektronix TDS7704B, 7 GHz, 20 GSa/s). The overall temporal response of the system has been measured to be Gaussian-shaped with a FWHM of 116 ps, when tested with a sup-picosecond laser pulse. The value is sufficient to resolve the temporal features of the probe pulse. As shown by Fig.1, a fraction of the probe laser beam is reflected from a glass plate before entering the cell, in order to be used as a reference pulse to measure the delay. The reference pulse is sent to the detection system together with the main part of the probe pulse that exits the cell. The lengths of the two optical paths are adjusted in order to be able to detect the two pulses with the same detector without temporal overlapping. With this configuration,

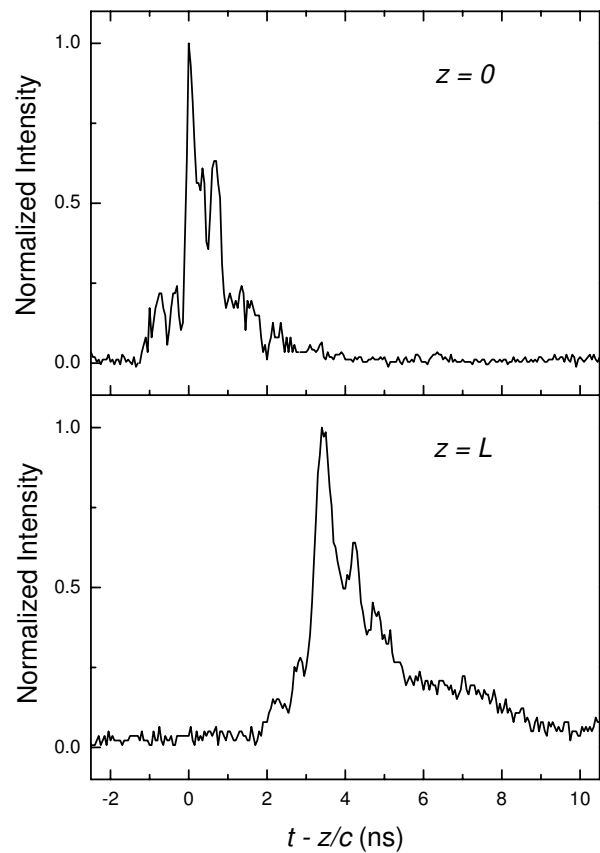


FIG. 2: The upper and lower graphs show, respectively, the probe laser pulse at the input and at the output of the cell. Relative delay, transmission and likeness for this pulse are, respectively, $\Delta t = 3.4$ ns, $T = 0.57$ and $\mathcal{L} = 0.90$.

several measurements of temporal delay and energy absorption of the probe pulse were realized changing the control laser intensity.

Figure 2 shows an example of a comparison between a pulse as it enters (top graph) and exits (bottom graph) the cell. It can be seen that the main temporal features of the pulse are preserved after propagation through the cell. A moderate broadening of these features can be observed, indicating that the spectral wings of the probe field are slightly affected by the propagation through the delay line. In Fig. 3(a) the measured transmission T is reported as a function of the measured relative delay Δt due to the effect of EIT. We report pulse delays up to $\Delta t = 8.9$ ns. The experimental data are in good agreement with the theoretical curve [14]:

$$T = \exp(-2\gamma_{13}\Delta t) \quad (1)$$

where γ_{13} is the decoherence rate of the two-photon transition 1-3. A best fit provides for the dephasing rate the value $\gamma_{13} = 1.1 \times 10^8 \text{ rad/s}$, which is compatible with the combined contributions of radiative decay and collisional effects due to residual gases in the cell.

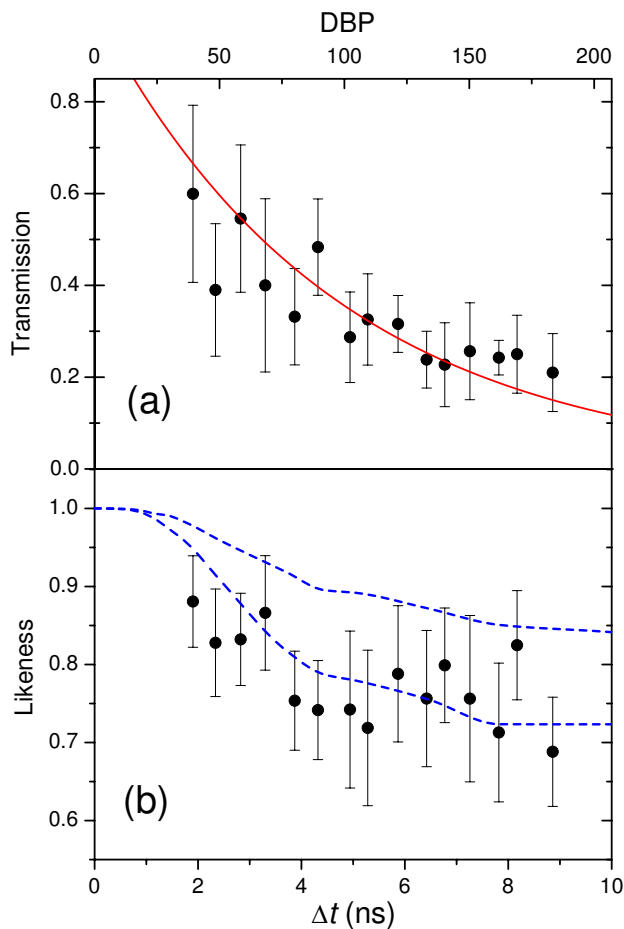


FIG. 3: Transmission (a) and likeness (b) as a function of the pulse delay. The full circles with error bars are the experimental data. In (a) the continuous curve is a fit of the experimental data using the theoretical expression 1. In (b) the dashed lines represent the results of a theoretical calculation (see text for details).

An important parameter characterizing optical delay lines is the *delay-bandwidth product* DBP , given by the product of the spectral bandwidth $\delta\omega$ of the optical field carrying the information, times the temporal delay accumulated upon propagation in the line: $DBP = \Delta t \times \delta\omega$. In the top-horizontal axis of Fig. 3 we report the very high values of DBP that we obtain in our experiment (up to a maximum of 183). Besides the DBP , another important parameter is the temporal shape distortion suffered by the optical pulse. For single-mode smooth pulses, the FWHM temporal width is an adequate parameter to describe their temporal shape and the broadening factor a commonly used parameter to characterize the tempo-

ral distortion suffered upon propagation in the line. On the contrary, for laser pulses with the multi-peak temporal structure shown in Fig. 2, a much more adequate parameter is the *likeness* \mathcal{L} , defined as:

$$\mathcal{L}(I_1, I_2) = 1 - \frac{\int_{-\infty}^{+\infty} [I_1(t) - I_2(t)]^2 dt}{\int_{-\infty}^{+\infty} I_1^2(t) dt + \int_{-\infty}^{+\infty} I_2^2(t) dt} \quad (2)$$

where for our case $I_1(t) = I_p(z = 0, t)$ and $I_2(t) = I_p(z = L, t - L/c - \Delta t)/T$. With this definition, \mathcal{L} varies between 0 and 1 and its value for two identical pulses is $\mathcal{L} = 1$. This quantity is reported as a function of the relative delay Δt in Fig. 3(b), where the experimental data (full circles) are compared with the results of a numerical simulation. The numerical results are obtained by integrating the probe pulse propagation equation for constant coupling field in the presence of Doppler broadening [15]. The spectrum of the input probe field is generated as the superposition of a series of Gaussian modes with a 3.3-GHz wide Gaussian envelope. The modes are separated from each other by 0.5 GHz and each of them has a width of 0.15 GHz with a different random constant phase. With these choices the temporal shape of the obtained pulses reproduce quite well the main features of the real pulses generated by the multimode dye laser. We observe that the theoretical values of \mathcal{L} for a given Δt are ‘dispersed’ over a broad range due to the different spectral phase of each pulse at the cell input. In order to show these variations, we chose to report two curves (dashed lines in Fig. 3(b)), representing the values $\mathcal{L}_m + \sigma_{\mathcal{L}}$ and $\mathcal{L}_m - \sigma_{\mathcal{L}}$, where \mathcal{L}_m and $\sigma_{\mathcal{L}}$ are the mean value and the standard deviation resulting from the propagation of 500 pulses with different randomly generated initial spectral phases. The experimental data are in satisfactory agreement with the theoretical calculations, particularly so if we consider that the theoretical curves in Fig. 3(b) do not use any free parameter.

In summary, we presented the first experimental demonstration of controllable delay of large-spectral-bandwidth multimode laser pulses using EIT. We managed to delay by several nanoseconds and with limited temporal distortion pulses with an input spectral bandwidth of 3.3 GHz. These results provide useful information about the potential of systems based on EIT for the purpose of designing all-optical delay lines and buffers with very fast temporal switching.

All the experimental work reported in this study was carried out in the laboratories of the Department of Physics of the University of Florence.

[1] M. Fleischhauer, A. Imamoglu, and J. P. Marangos, “Electromagnetically induced transparency: Optics in

coherent media”, Rev. Mod. Phys. **77**, 633 (2005)

[2] M. S. Bigelow, N. N. Lepeshkin, and R. W. Boyd, “Ob-

- servation of Ultraslow Light Propagation in a Ruby Crystal at Room Temperature”, *Phys. Rev. Lett.* **90**, 113903 (2003)
- [3] P. Palinginis, F. Sedgwick, S. Crankshaw, M. Moewe, C. J. Chang-Hasnain, “Room temperature slow light in a quantum-well waveguide via coherent population oscillation”, *Opt. Express* **13**, 9910 (2005)
- [4] K. Y. Song, M. G. Herráez, Miguel González, and L. Thévenaz “Long optically controlled delays in optical fibers”, *Opt. Lett.* **30**, 1782 (2005)
- [5] M. D. Stenner, M. A. Nedfield, Z. Zhu, A. M. C. Dawes and D. J. Gauthier, “Distortion management in slow-light pulse delay” *Opt. Express* **13**, 9995 (2005).
- [6] Y. Okawachi, M. S. Bigelow, J. E. Sharping, Z. Zhu, A. Schweinsberg, D. J. Gauthier, R. W. Boyd, and A. L. Gaeta “Tunable All-Optical Delays via Brillouin Slow Light in an Optical Fiber”, *Phys. Rev. Lett.* **94**, 153902 (2005)
- [7] J. Sharping, Y. Okawachi, and A. Gaeta, “Wide bandwidth slow light using a Raman fiber amplifier”, *Opt. Express* **13**, 6092 (2005)
- [8] D. Dahan, and G. Eisenstein, “Tunable all optical delay via slow and fast light propagation in a Raman assisted fiber optical parametric amplifier: a route to all optical buffering”, *Opt. Express* **13**, 6234 (2005)
- [9] R. M. Camacho, M. V. Pack, and J. C. Howell, “Slow light with large fractional delays by spectral hole-burning in rubidium vapor”, *Phys. Rev. A* **74**, 033801 (2006)
- [10] R. M. Camacho, M. V. Pack, and J. C. Howell, “Low-distortion slow light using two absorption resonances”, *Phys. Rev. A* **73**, 063812 (2006)
- [11] R. M. Camacho, M. V. Pack, J. C. Howell, A. Schweinsberg, and R. W. Boyd “Wide-Bandwidth, Tunable, Multiple-Pulse-Width Optical Delays Using Slow Light in Cesium Vapor”, *Phys. Rev. Lett.* **98**, 153601 (2007)
- [12] R. Buffa, S. Cavalieri, and M. V. Tognetti, “Coherent control of temporal pulse shaping by electromagnetically induced transparency”, *Phys. Rev. A* **69**, 033815 (2004)
- [13] T.D. Raymond and A.V. Smith, “Injection-seeded titanium-doped-sapphire laser” *Opt. Lett.* **16**, 33 (1991)
- [14] A. Kasapi, Maneesh Jain, G.Y. Yin and S. E. Harris, “Electromagnetically Induced Transparency: Propagation Dynamics”, *Phys. Rev. Lett.* **74**, 2447 (1995)
- [15] R. Buffa, S. Cavalieri, M.V. Tognetti, “Temporal compression of short-wavelength laser pulses by coherent control in rare gases”, *Opt. Lett.* **29**, 2432 (2004)